This is an open access article distributed under the terms of the Creative Commons Attribution 4.0 International License (CC BY 4.0), which permits use, distribution, and reproduction in any medium, provided the original publication is properly cited. No use, distribution or reproduction is permitted which does not comply with these terms.

STRENGTH CHARACTERISTICS OF FE-SMA REINFORCEMENT IN RC BEAM WITH EXPERIMENTATION AND FINITE ELEMENT MODELING

Priyanka Jadhav[1], Archana Gite[2], Rajan L. Wankhade[3,*]

[1]Department of Civil Engineering, Terna Engineering College Nerul, Navi Mumbai, Maharashtra, India
[2]Department of Civil Engineering, Saraswati College of Engineering, Maharashtra, India
[3]Department of Civil Engineering, Netaji Subhas University of Technology, New Delhi, India

*E-mail of corresponding author: rajan.wankhade@nsut.ac.in

Priyanka Jadhav 0000-0001-9988-9353, Rajan L. Wankhade 0000-0002-6141-8924

Resume

The work presented here aims at investigating the feasibility of iron-based Fe-SMA (shape memory alloy) reinforcement as an alternative to conventional steel reinforcement. The conventional steel reinforcement shows large plastic strain, low resistance to corrosion, low resistance to fatigue and also inadequate recentering capability. As a result, advanced materials available in the form of superelastic (SE) shape memory alloy (SMA) are fabricated to form structural reinforcements. This FE-SMA mitigates the problem of long-lasting deflection by using its reversible stress-strain capability. This iron-based Fe-SMA may be stimulated between the temperatures of 90 to 150°C, with which it is possible to strengthen the reinforced concrete (RC) beams without any crucial damage. The stress-strain behavior in tension, corrosion resistivity, pull-out tests of Fe-SMA reinforcement and flexural strength of RC beam were evaluated experimentally. The FE-SMA exhibits recovery stresses of 250-300 MPa subjected to a temperature of 160°C. A comparison of load-carrying capacity of iron-based Fe-SMA reinforcement is also shown.

Article info

Received 9 December 2022
Accepted 28 February 2023
Online 12 April 2023

Keywords:

Fe-SMA
RC beam
flexural strength
stress-strain relationship

Available online: https://doi.org/10.26552/com.C.2023.043

ISSN 1335-4205 (print version)
ISSN 2585-7878 (online version)

1 Introduction

In recent years; researchers are focusing to employ the smart materials technology in composite structures. SMA characteristics and behavior of Fe-30Mn-1Si alloy as a single crystal were put forth by Sato et al. [1]. Reinforced cement concrete is one of the areas where SMA materials can be used. In reinforced concrete structures, we use conventional steel as reinforcement, which has its own deficiency in terms of structural response. This deficiency can be overcome by Shape Memory Alloy (SMA) bars. The SMA is an alloy, which has a property to regains its unique shape and size upon the removal of stress or by application of a temperature field [2]. The four basic types of SMA are: (a) copper-zinc (b) aluminum-nickel (c) copper-aluminum-nickel and (d) nickel-titanium (NiTi) alloys. These may also be fabricated by casting zinc, iron, copper and gold.

There exist two main groups of iron-based SMA's. The first group of it comprise Fe-Pt, Fe-Pd and Fe-Ni-Co, exhibiting the same features as Ni-Ti, thermoelastic martensitic transformations with a precise thermo hysteresis. The second group comprises alloys of Fe-Ni-C and Fe-Mn-Si, showing extensive thermal hysteresis in transformation.

Effectiveness of equiatomic and near-equiatomic titanium-nickel alloys and compositions showing shape memory and superelastic behavior are described by Duerig and Pelton [3]. SMA reinforcements and composites are mostly employed as self-restoration of structural members in various applications [4-9]. Janke et al. [10] emphasized the behavior of SMAs in terms of super elasticity, martensite damping and variable stiffness to be used as highly non-linear material. Song et al. [11] explored a review of use of the SMA for active-passive and semi-active controls of reinforced cement concrete RCC structures. Alam et al. [12] predicted analytically the seismic response of superelastic SMA in RCC structural components. It became necessary to model the SMA reinforcements properly to evaluate the structural response in tension and compression [13-16]. Hence, the passive smart self-repairing concrete beams by incorporating SMA wires and fibers are also found to be fabricated [17]. Mathematical models are developed to examine accurate strain-temperature behavior of SMA actuators [18]. Both experimental investigation and finite element modeling is an effective approach to examine the SMA rebar characteristics [19-20]. Nehdi et al. [21] focused on casting corrosion-resistant RCC beam-column with required energy dissipation (seismic) through SMA FRP fiber reinforced polymer hybrid beam-column joint and FRP ties. Experimental results showed that over strength factor of the SMA-RC frame was analogous to that of the steel RC frame with a difference of 8%. SMA frame has ductility at least 16% less compared to that of steel RC frames whereas for steel-SMA frames it ranges from 8 to 18% less from that of steel RC frames. Properties and application of iron based SMA alloys are given in literature [22].

Speicher et al. [23] investigated the response of beam-to-column connection frame in NiTi-SMA. These SMA alloys are also effective in controlling the response of structure in seismic excitations [24]. Paul and Saha [25] found out the load-carrying capacity of RC bridge longitudinal girder having the T-beam by providing SMA bars in place of conventional steel reinforcement. Abdulridha et al. [26] examined the influence of various loads on the NiTi SMA reinforced beam in comparison to conventional steel reinforcement. Experimental examination on performance of the RC structural members, having hybrid SMA and FRP bars as reinforcement, subjected to seismic loading, is found to be useful [27-28]. Choi et al. [29] examined the influence of using the welded SMA rings on a column to reduce development of micro cracks. Results show that composite reinforcement bars, fabricated from SMA alloys, are more effective in controlling the seismic behavior of structures [30]. A similar type of work has also been put forth by employing pizolaminated beams and plates for structural control [31-34]. Mechanical properties are studied to investigate the load recovery in the SMA hybrid components [35-36]. Cladera et al. [37] stated a state of the art for characteristics and employed the iron-based SMA to study properties including recovery stress, weldability, resistance to corrosion and workability of iron-based SMA.

Czaderski et al. [38] opened up the feasibility of iron-based SMA strips for strengthening the prestressed concrete structures. Sepulveda et al. [39] experimentally verified a prototype of a partially restrained connection using the copper-based SMA. Malagisi et al. [40] modeled smart concrete beams with actuating SMA. In the pre-stressed concrete SMA reinforcements have more advantages due to their stress recovery property [41]. Some smart composites manufactured with pizolaminated structures are also effective in controlling structural response [42]. Bendine and Wankhade [43] employed finite element modeling to study characteristics of actuated piezolaminated smart beams. Hence, dynamic excitations of actuated beams and plates can also be controlled by use of such smart materials [44]. Fatigue properties of Fe-28Mn-6Si-5Cr-0.5Nbc alloy are examined for its utility in structural applications [45]. Furthermore, the genetic algorithm is developed to find optimal locations of active materials in the composites [46-47]. Actuation and sensing behavior of smart composites have been demonstrated to study control response of beams and plates [48-49].

Based on the above scenario, we performed experimental work to investigate the performance analysis of conventional steel and Fe-SMA rebar, stress-strain behavior in tension, corrosion resistivity and pull-out responses of the Fe-SMA reinforcement in comparison to the conventional reinforcement. An experimental research work is proposed utilizing the Fe-SMA as reinforcement in reinforced concrete (RC) beam to compare the flexural strength with conventional steel reinforcement in RC beam and results are validated using ANSYS 16. Coarse and fine aggregates in RC beam are used conforming to IS 383: 1970 standard specification [50]. Further for test on reinforcement bars IS 11309: 1985 standard is followed to conduct pull-out test [51]. A comparison of load-carrying capacity of Fe-SMA reinforcement using ANSYS 16 is carried out to obtain more durable reinforcement having longer lifetime than that of conventional reinforcement. The comparative study between the costs of various types of reinforcing bars used for construction purposes is carried to obtain cheaper alloys as an alternative to expensive NiTi alloys.

2 Phenomenon of iron-based shape memory alloy (Fe-SMA)

Basically, the SMAs exhibit the complaisant tendency of memorizing their shape after being deflected, either quickly upon stress removal or under thermal effect.

The SMAs comprise more than one crystal structure like other alloys and to be termed as polymorphism. Temperature and external loading both govern the preponderating nature of crystal structure in such polycrystalline metals and alloys.

The tendency of SMAs to be active and stronger in the austenite phase and in the martensite phase, i.e. at lower temperatures it is feeble, can be employed effectively in RC members. The transition temperature of SMAs varies from, about -50 °C to 166 °C, depending upon their compositions. It shows a simplified two-dimensional representation of the material’s crystalline arrangement.

Phase transformation in SMA occurs at four characteristic temperatures as (1) the austenite

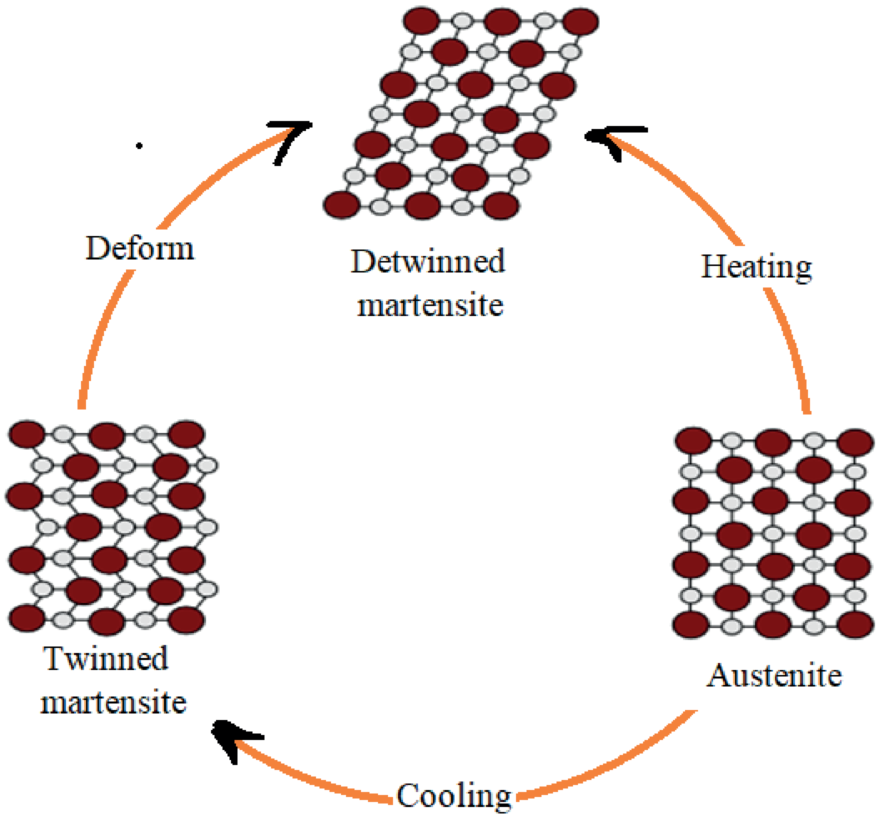

Figure 1 *Different phases of shape memory alloys*

start temperature As, where the material starts to transform from twinned martensite to austenite, (2) austenite finish temperature Af, where the material is completely transformed to austenite, (3) martensite start temperature Ms, where austenite begins to transform into twinned martensite, (4) martensite finish temperature Mf, where the transformation to martensite is completed. Figure 1 depicts these transformation phases as temperatures increase with applied stress.

2.1 The martensitic transformation

Shape Memory Effect (SME)

The shape memory effect is the capability of SMA material to achieve its pre-deformed shape after being deformed by means of a thermal effect. Below the Mf temperature, the SMA remains in the twinned martensite phase. After the application of loading above the critical level, the material transforms to a detwinned martensite phase to maintain this phase even after the stress removal. Above the Af temperature, if the SMA material is heated, it re-achieves its original shape/ size. Hence, warming the material above Af results in the gaining of the austenite phase and thus a complete shape recovery. By the consequent cooling, the SMA transforms to the initial twinned martensite phase without any enduring deformation.

The super elastic effect (SE) may be termed as the restoration of large strain by virtue of the stress-induced martensitic phase transformations under definite temperature. The SMA remains in its austenite phase at a temperature above Af. After the application of higher stress to the material in the austenite phase, the SMA mold into the detwinned martensite. A partial shape recovery can be seen if the temperature remains in between Af and As. In addition, the martensitic transformations may not be brought about by applied stress if the temperature was above the critical temperature (Md), as the material may get stabilized in the austenite phase only.

2.2 Advantages of Fe-SMA over conventional reinforcement

The Fe-SMA exhibits an immense temperature transformation hysteresis with a higher elastic stiffness. In addition, as compared to the conventional steel reinforcement their corrosion resistance and weld ability are superior.. The shape memory alloys are benefited from the potency of recentering and recovering more than 80% of the induced strains; high modulus of elasticity; similar behavior in tension and compression. It is again used for making machined components such as bolts; high resistance against corrosion and with high resistance against fatigue as compared to

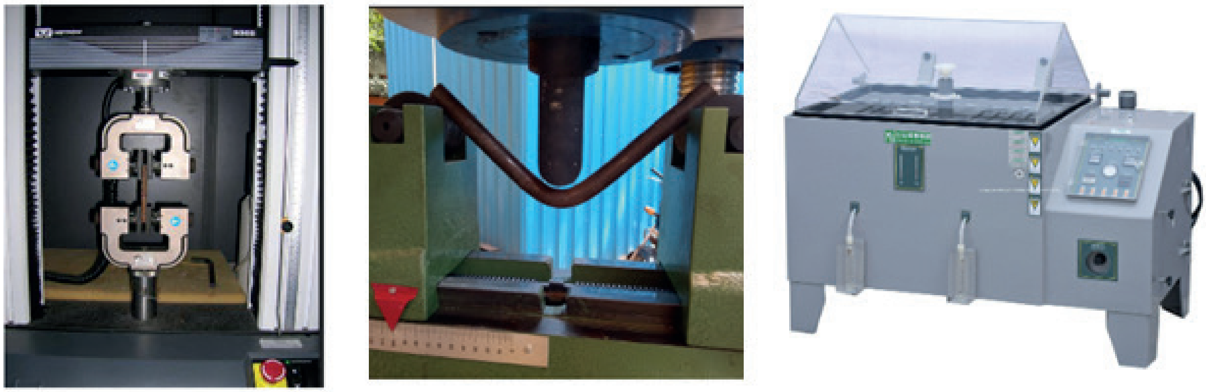

(a) (b) (c)

***Figure 2** (a) Tensile test; (b) Bend test; (c) Salt spray test*

conventional reinforcement. After considering all the options, shape memory alloys can be considered as an alternative reinforcement over the conventional one, by finding optimum benefits, while neglecting the maximum possible deficiencies of the same.

The primary aim of the present study is to investigate the performance of fabricated Fe-SMA reinforcing bars over conventional reinforcing bars along with comparison of the RC beams with and without Fe-SMA reinforcement, both experimentally and analytically using ANSYS. Based on the presented literature review, the following objectives have been drawn:

3 Experimental study

The experimental study is designed to facilitate the investigation on the feasibility of Fe-SMA reinforcing bars in RC structures in terms of tensile strength, corrosion resistivity, load-carrying capacity and pull-out resistance. Fe-SMA reinforcing bars were fabricated with optimum gradation [Iron (Fe)-72%, Manganese (Mn)-6.57%, Silicon (Si)-0.21%, Chromium (Cr)-15.82%, Nickel (Ni)-4.08%)] of 10mm diameter, on which chemical test was carried out as per IS 9879:1998 to achieve desired optimum gradation [52]. IS 9103: 1999 standard is also used for concrete admixtures-specifications [53]. Tensile test, bend test and corrosion test were carried out on mild steel, TOR steel and Fe-SMA reinforcing bars and shown in further sections. Flexural test under the three-point bending test condition was performed on RC beams with conventional reinforcement, Fe-SMA reinforcement and combination of conventional and Fe-SMA reinforcement. Pull-out test on concrete with mild steel, TOR steel and Fe-SMA reinforcing bars was performed to achieve greater bond strength.

3.1 Test on reinforcing bars

The Fe-SMA reinforcement was fabricated from Iron, Manganese, Silicon, Chromium and Nickel as stated. This gradation helps to verify the strength of bars under different tests. Hence, the tensile test, bend test and salt spray test were performed on TOR steel, mild steel and Fe-SMA reinforcing bars respectively as shown in Figures 2(a)-2(c), respectively.

3.2 Test on RC beams and cubes

A Material and mixes
Concrete

The concrete is formed with different ingredients and materials. The admixture used was MasterRheobuild-1124 superplasticizer, 2% by mass of cementitious material as per IS 9103:1999 standard [53]. The specific gravity of the admixture was found to be 1.145. Reinforcements used for beam specifications were based on IS 1786: 2008 standard specifications required for concrete [54]. The mix proportion used was 1:2:2.87 with a water-cement ratio used was 0.35 as per IS 10262:2009 standard [55]. ASTM B117: 2011 standard guidelines are employed for different test conditions and method [56]. The raw material, consisting of Ordinary Portland cement of 53 grade, conforming to Indian Standard IS 12269:2013, was used throughout the experimental program [57]. The minimum fineness was 225m^2/kg. The standard consistency was 30.5%, whereas the initial and final setting times were 30 min and 600 min, respectively. The specific gravity of cement was 3.14 and its compressive strength after 28 days was 53 MPa. The coarse aggregate-I (CA-I) and coarse aggregate-II (CA-II) of maximum size 10mm and 20mm, respectively, were used.. The bulk density of CA-I and CA-II was 1.5gm/cm^3 and 1.589 gm/cm^3, respectively. The specific gravity of CA-I and CA-II was found to be 2.8 and 2.82, respectively. The crushed sand and natural sand conforming to zone-II is used with bulk density of 1.712 gm/cm^3. The specific gravity of crushed sand was found to be 2.76. The cement content was 384 kg/m^3..

Table 1 Final Batch weight in kg/m³ of concrete and material and mechanical property of Fe-SMA

Cement (kg/m³)	PFA (kg/m³)	CA-II (kg/m³)	CA-I (kg/m³)	CFA (kg/m³)	Water (kg/m³)	Admixture (kg/m³)	Total (kg/m³)
384	96	613	408	755	220	6.24	2482

Reinforcement	Material and mechanical property	Range
Fe-SMA	Elastic Modulus (GPa)	75-165
	Yield Stress (MPa)	400-550
	Failure Strain (%)	40
	Optimum Prestrain (%)	2-4
	Activation Temperature (°C)	160-500
	Recovery Stress (MPa)	130-580

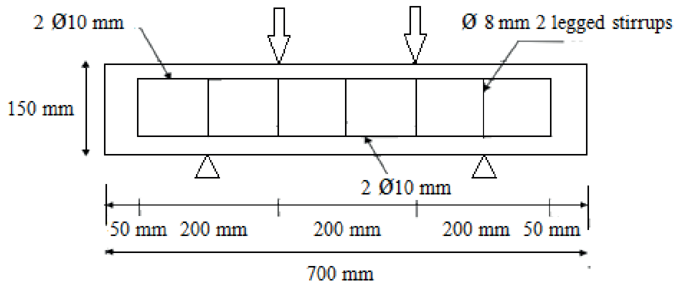

(a)

(b)

***Figure 3** Flexural test (a) Loading and reinforcement details (b) setup*

Reinforcement

A bilinear stress-strain curve has been used for the steel behavior. The values of elastic modulus and Poisson's ratio of steel are 200 GPa and 0.3, respectively. The steel is assumed to have a yield strength of 500 MPa. The Fe-SMA reinforcement with optimum gradation is used. Table 1 shows the mix design used in this study.

B Experimental setup for the three-point bending test

The RC beams were cast with the dimension of 150mm x150mm x700mm. Results from the three-point bending test are obtained for three combinations.

a) Conventional reinforcement of 2Ø10 mm at the top and 2Ø 10 mm at the bottom,
b) Fe-SMA reinforcement 2Ø 10 mm at the top and 2Ø 10 mm at the bottom,
c) Combination of conventional reinforcement Ø10 mm at the top, Ø10 mm at the bottom and Fe-SMA reinforcement Ø10 mm at the top with Ø10 mm at the bottom.

The thickness of the layer cover was 25 mm. The axial distance of the stirrup was 100 mm. The load applied was up to 100 kN, as per IS 516:2021 standard [58], flexural test using a three-point bending test setup was carried out as shown in Figure 3.

The test specimen for pull-out test was basically

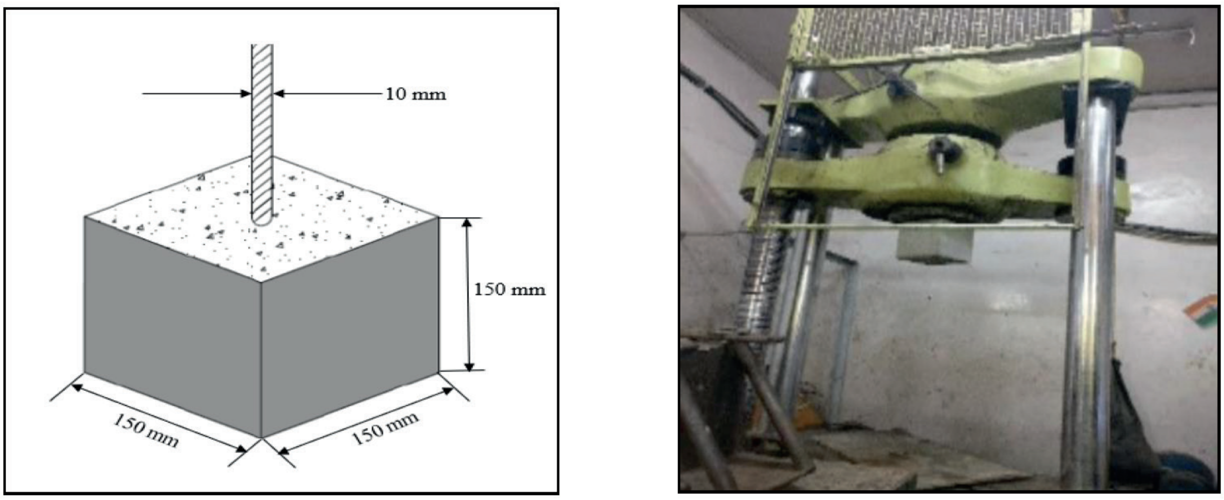

Figure 4 *Pull-out test (a) Specimen details (b) setup*

Table 2 *Material types and element types of the finite element model*

Material types	ANSYS elements
Concrete	Solid 65
Steel support	Solid 45
Steel reinforcement (main r/f and stirrups)	Link 8
Fe-SMA reinforcing bars	Link1

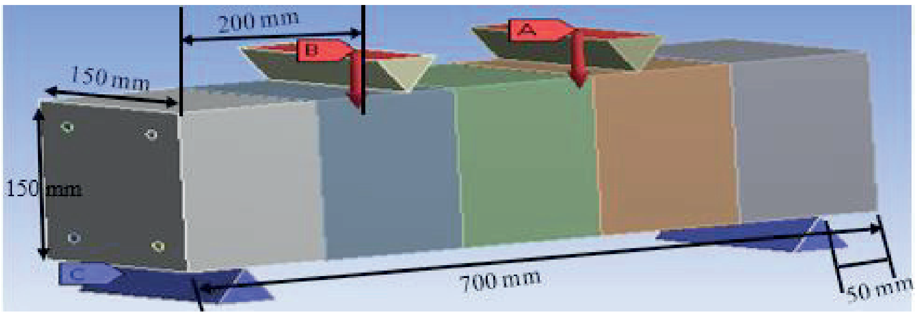

Figure 5 *FE model in ANSYS for RC beam reinforced with a combination of conventional reinforcement and Fe-SMA reinforcing bars under the four-point bending test condition*

a concrete cube of 150 mm x 150 mm x 150 mm dimension with a bar embedded coaxially. The upper end of the bar under test was projected up to the length of 500 mm. Double nuts were fitted in it above the 400 mm high spring-return central-hold jack, as shown in Figure 4. Therefore, the ultimate pullout force is directly proportional to the compressive strength.

4 Analytical study

4.1 Finite element modeling

The static analysis is performed on a concrete beam modeled with dimensions 150 mm x 150 mm x 700 mm. The beam is reinforced with conventional reinforcement as well as with Fe-SMA reinforcement for undergoing flexural test under the four-point bending test conditions. To reduce the time for analysis, half RC beam was modeled. Thus, Figure 5 shows arrangement of reinforcement in the beam. Results from the four-point bending test are obtained for three combinations same used in the experimental program, (a) conventional reinforcement of 2Ø10 mm at the top and 2Ø 10 mm at the bottom, (b) Fe-SMA reinforcement 2Ø 10mm at the top and 2Ø 10 mm at the bottom and (c) combination of conventional reinforcement Ø10 mm at the top, Ø10 mm at the bottom and Fe-SMA reinforcement Ø10 mm at the top with Ø10 mm at the bottom. Table 2 summaries the material types and element types of the model in ANSYS 16.

4.2 Mesh, loading and support condition

The RC beam, with and without Fe-SMA reinforcement, model with a particular mesh sizing is calculated in such a way that the better results are

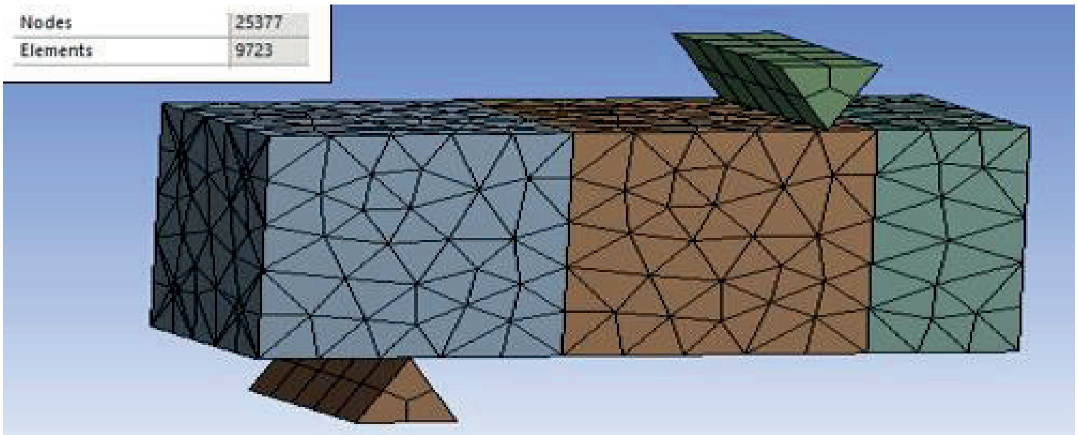

Figure 6 *Mesh for static analysis under the four-point bending test of RC beam reinforced with and without Fe-SMA reinforcement*

obtained from the elements. The inherent assumption is that there is full displacement compatibility between the reinforcement and the concrete and that no bond slippage occurs. Figure 6 represents the model of the beam under consideration with its meshing in ANSYS. Proper mesh and elements are demonstrated for convergence criteria. At first, the beam is modeled with normal reinforcement and solved to get the results. In the next step, the same beam is modeled with Fe-SMA reinforcement for comparison. Only half of the beam is shown here with the FE mesh in the enlarged view. Displacement boundary conditions are needed to constrain the model to get a unique solution. The support was modeled as roller support at one end and the other end as a hinged support. Loading is applied as per the four-point bending test for flexure.

5 Results and discussion

This paper focuses on feasibility of the Fe-SMA reinforcing bars as an alternative to conventional reinforcement in structural engineering. Fabricated Fe-SMA reinforcing bars were used for experimentation. Tensile test, bend test and corrosion test were carried out on mild steel, TOR steel and Fe-SMA reinforcing bars to achieve mechanical and corrosion properties. The pull-out test on concrete with mild steel, TOR steel and Fe-SMA reinforcing bars was also performed to check the bond strength. Flexural test under three-point bending test condition was performed on RC beams with conventional reinforcement, Fe-SMA reinforcement and a combination of conventional reinforcement both experimentally and then analytically in ANSYS 16. The results are compared for conventional and Fe-SMA reinforcement with respect to the flexural strength of the beam. To interpret a comparison between the conventional reinforcement and Fe-SMA reinforcement, with respect to the stress, deformation and fatigue properties of reinforcing bars were evaluated, as well. Based on this scenario, results are presented.

5.1 Chemical test on Fe-SMA reinforcing bars

The chemical test is carried out on Fe-SMA reinforcing bars and results are provided further. The main elements of Fe-SMA bars are iron, manganese, silicon, chromium and nickel. The addition of manganese at 6.57% and silicon with 0.21% allows the shape memory effect to occur. The addition of chromium with 15.82% and nickel with 4.08% improves its corrosion resistance and improves effectiveness in restraining.

5.2 Tensile test on reinforcing bars

A tensile test is carried on mild steel, TOR steel and Fe-SMA reinforcing bars as per ASTM A370 [59]. Table 3 shows results related to the tensile test on reinforcing bars. Stress-strain graphs for mild steel, TOR steel and Fe-SMA reinforcing bars, Figures 7 (a), (b) and (c), reveal many properties like 0.2% proof stress and ultimate tensile strength, including data to establish the modulus of elasticity of mild steel, TOR steel and Fe-SMA, respectively. Figure 7 (c) shows flag shaped curve, which indicates at the loading stage, SMA takes a large level of strain as the stress remains fairly constant and then at unloading the SMA recovers strain at a lower stress stage. Figures 8 (a), (b) and (c) show the cup and cone fracture of TOR steel, mild steel and Fe-SMA reinforcing bars after the tensile test, respectively. Table 3 shows 0.2% proof stress for mild steel, TOR steel and Fe-SMA are 681 MPa, 504 MPa, 868 MPa, respectively. This indicates that there is a 22% and 42% precedent beginning of nonlinear deformation of Fe-SMA as compared to mild steel and TOR steel, respectively.

The ultimate tensile strength of steel, mild steel and Fe-SMA are 743 MPa, 621 MPa and 1037 MPa, respectively. This indicates that Fe-SMA has 40% and 29% maximum capacity to withstand while being stretched or pulled before breaking as compared to mild steel and TOR steel respectively. The modulus of

Table 3 *Tensile test on reinforcing bars*

Specimen	Dia. (mm)	Maximum Load (kN)	0.2% proof stress (MPa)	U.T.S (MPa)	Modulus (GPa)
TOR steel	10	45.81	504	621	187
Mild steel	10	58.09	681	743	200
Fe-SMA	10	81.09	868	1037	208

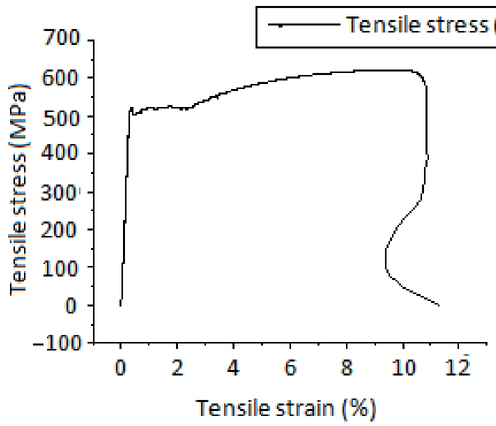

(a)

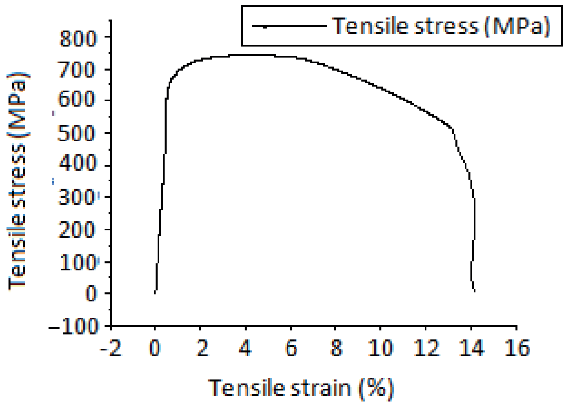

(b)

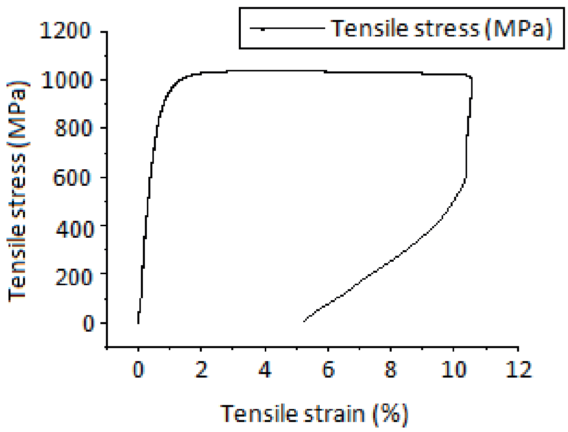

(c)

Figure 7 *Stress-Strain curves for (a) mild steel (b) TOR steel (c) FE-SMA*

Figure 8 *Specimen after the tensile test (a)mild steel (b) TOR steel (b) Fe-SMA*

Table 4 Bend test of reinforcing bars

Specimen	Diameter (mm)	Bend	Remark
Mild steel	10	4D	Satisfactory
TOR steel	10	4D	Satisfactory
Fe-SMA	10	4D	Satisfactory

Table 5 Corrosion test of reinforcing bars

Specimen	Dia. (mm)	Period (h)	Observation
Mild steel	10	24	Red pitting observed
TOR steel	10	24	Red pitting observed
Fe-SMA	10	24	Slightly red pitting at cutting edge

Table 6 Pull-out test

Case	Material	Diameter of bar (mm)	Maximum Load (kN)	Bond strength (N/mm^2)
1	RC cube with mild steel	10	22.6	0.72
2	RC cube with TOR steel	10	22.8	0.73
3	RC cube with Fe-SMA	10	15.1	0.48

elasticity for mild steel, TOR steel and Fe-SMA are 200 GPa, 187 GPa and 208 GPa respectively. This indicates that Fe-SMA is for 4% and 10% stiffer material, as compared to mild steel and TOR steel, respectively.

5.3 Bend test on reinforcing bars

The bend test was a simple and inexpensive qualitative test that can be used to evaluate both the ductility and soundness of a material. The bend test is carried out on mild steel, TOR steel and Fe-SMA reinforcing bars to suggest the suitability for concrete structures. Figure 9 shows the results of the bend test on mild steel, TOR steel and Fe-SMA, respectively. The results of this test show satisfactory remarks, which indicates that none of the material failed under pressure as no fracture occurred on mild steel, TOR steel and Fe-SMA. It is observed that during the test there no crack has developed in TOR steel, mild steel nor the Fe-SMA reinforcement, after undergoing a 180° bend. Hence, those reinforcement bars can be effectively used with concrete as a ductile material further loaded with bending forces. However, when those reinforcements are used in concrete, cracks, which are measurable, get developed in concrete, while with use of the Fe-SMA, these cracks in concrete get diminished and recovered due to the self-healing properties. Table 4 shows the bend test results and their remarks.

5.4 Corrosion test on reinforcing bars

Corrosion test was carried out on mild steel, TOR steel and Fe-SMA reinforcing bars and the results were compared. Table 6 shows the results of the corrosion test mild steel, TOR steel and Fe-SMA respectively. Figure 10 shows specimens before and after the test. Table 5 shows that in the salt solution of 5% (in weight) of NaCl, (more than seawater, which is only 1.8% to max 3%) maintained at 35 ºC with pH ranges from 6.5 to 7.2 for 24 h, red pitting was observed on the mild and TOR steel, whereas for the Fe-SMA reinforcing bars slightly red pitting was observed at the cutting edge. These results indicate that the Fe-SMA reinforcing bars are more corrosive resistant than the mild and TOR steels.

5.5 Pull-out test

The pull-out test is carried out on reinforcing concrete embedded with mild steel, TOR steel and Fe-SMA reinforcing bars to verify the maximum load and bond strength. Figure 11 shows specimens after the pull-out test. Table 6 shows the maximum load of 22.6 kN, 22.8 kN and 15.1 kN acted on a cube reinforced with mild steel, TOR steel and Fe-SMA reinforcing bars respectively. Similarly, bond strengths were observed as 0.72 N/mm^2, 0.73 N/mm^2, 0.48 N/mm^2, for cubes reinforced with mild steel, TOR steel and Fe-SMA reinforcing bars, respectively. This indicates that the maximum load and bond strength of a cube embedded with Fe-SMA reinforcing bars is 34% smaller than mild and TOR steel. Thus, the bond strength is proportional to the contact surface of the steel to the concrete. A deformed reinforcing bar adheres better than a plain one because it has a greater bearing surface. The rougher the surface of the steel, the better it adheres to concrete. Thus, steel with a light, firm layer of rust is

(a) (b) (c)

Figure 9 *Specimens after bend test (a) mild steel (b) TOR steel (c) Fe-SMA*

(a) (b) (c)

Figure 10 *Reinforcing bars sample before and after corrosion test (a) mild steel (b) TOR steel (c) Fe-SMA*

Table 7 *Comparison of Flexural Strengths for RC beams reinforced with Conventional and FE-SMA*

Case	Reinforced concrete beam	Beam size (mm)	Maximum Load (kN)	Flexural strength (MPa)	
				Experimental results	Analytical results
1	Conventional reinforcement #2-10 mm Ø (top) #2-10 mm Ø (bottom)	150 x 150 x 700	71.48	12.65	12.43
2	Fe-SMA reinforcement #2-10 mm Ø (top) #2-10 mm Ø (bottom)	150 x 150 x 700	88.81	16.08	15.89
3	Conventional reinforcement #1-10 mm Ø (top) #1-10 mm Ø (bottom) Fe-SMA reinforcement #1-10 mm Ø (top) #1-10 mm Ø (bottom)	150 x 150 x 700	73.28	13.04	12.94

superior to clean steel; however, steel with loose or scaly rust is inferior.

5.6 Flexural test on the RC beams

Flexural test under the four-point bending test condition is carried out on RC beams experimentally to compare the flexural strength of RC beams with and without Fe-SMA reinforcement and the same results are validated using ANSYS 16. Table 7 shows the experimental and analytical results of RC beams with and without Fe-SMA reinforcement. Figures 12 (a), (b) and (c) show the flexural strength acting on RC beam with and without Fe-SMA reinforcement obtained from analytical results using ANSYS.

Table 7 shows that experimental results for the flexural strength of RC beams, with and without Fe-SMA reinforcement, are in good agreement with the analytical results for the flexural strength of RC beams with and without Fe-SMA reinforcement. The flexural strength of the RC beam reinforced with Fe-SMA and a combination of Fe-SMA and conventional reinforcement is observed to be 16.08 MPa and 13.04 MPa is 22% greater than the RC beam reinforced with conventional reinforcement. There is a marginal increase of 3% in the flexural strength of the combination of conventional reinforcement and Fe-SMA. This proves that Fe-SMA can withstand in severe conditions for longer period, as compared to conventional reinforcement.

5.7 Total deformation of RC beam

Total deformation is carried out on RC beams with and without Fe-SMA reinforcement, both experimentally and analytically. Figure 13 (a) shows the crack closure of the RC beam with Fe-SMA reinforcement at the maximum deflection is 0.53 mm and after the unloading it is 0.13 mm. Even if there was a marginal increase in total deformation of the RC beam with Fe-SMA reinforcement, it shows strain recovery of 75%. This results in crack vanishing in the RC beam with Fe-SMA reinforcement, as shown in Figure 13 (b). Figures 14 (a), (b) and (c) represent the total deformation on the RC beams with and without the Fe-SMA reinforcement. Analytical results show that the total deformation of Fe-SMA reinforcement is 0.04897 mm, which is marginally higher than that of the conventional reinforcement and a combination of conventional and Fe-SMA reinforcements, which is observed to be 0.03879.

5.8 Load-strain response and recovery stress

Further, for measuring the recovery strain of the

(a) *(b)* *(c)*

Figure 11 *Pull-out test (a) mild steel (b) TOR steel (c) Fe-SMA*

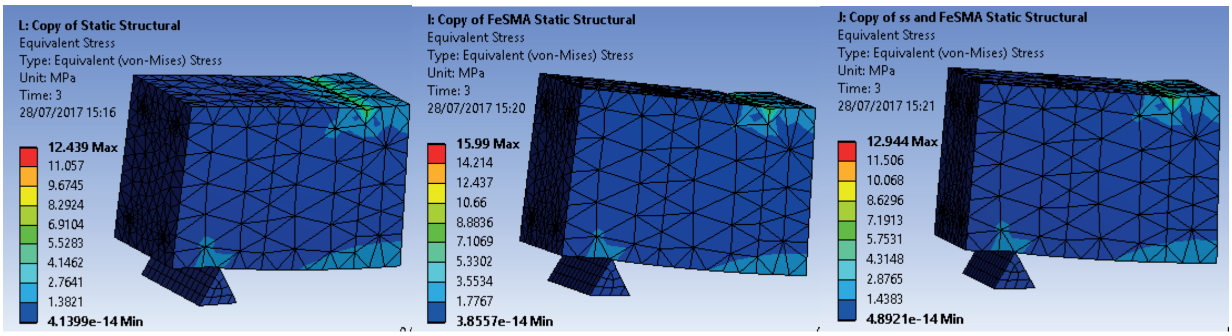

(a) *(b)* *(c)*

Figure 12 *Flexural strength on RC beam (a) conventional reinforcement (b) Fe-SMA reinforcing bars (c) combination of conventional reinforcement and Fe-SMA reinforcement*

(a) (b)

***Figure 13** Crack behavior of RC beam with Fe-SMA reinforcement (a) at maximum deflection (b) recentering of RC beam with Fe-SMA reinforcement after unloading*

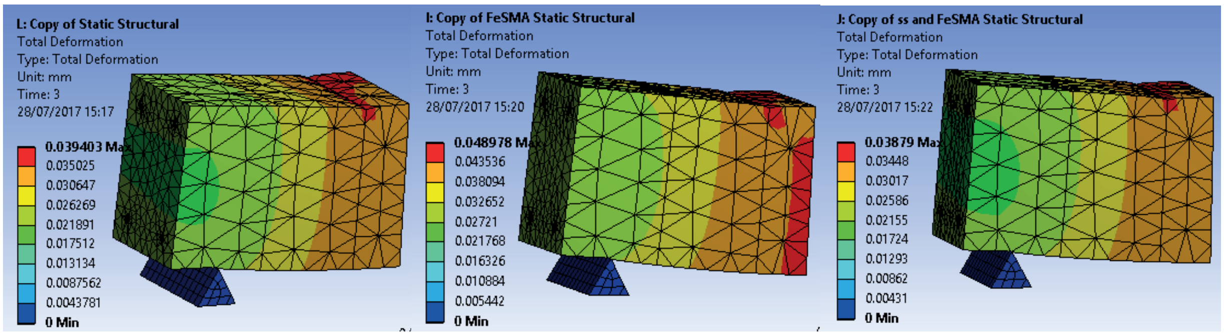

(a) (b) (c)

***Figure 14** Total Deformation on RC beams (a) conventional reinforcement (b) Fe-SMA reinforcing bars (c) combination of conventional reinforcement and Fe-SMA reinforcement*

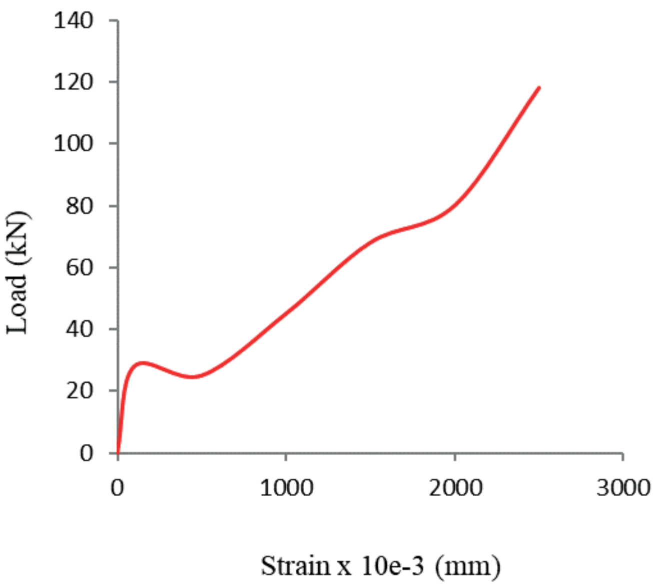

***Figure 15** Load-strain response of the Fe-SMA reinforcement*

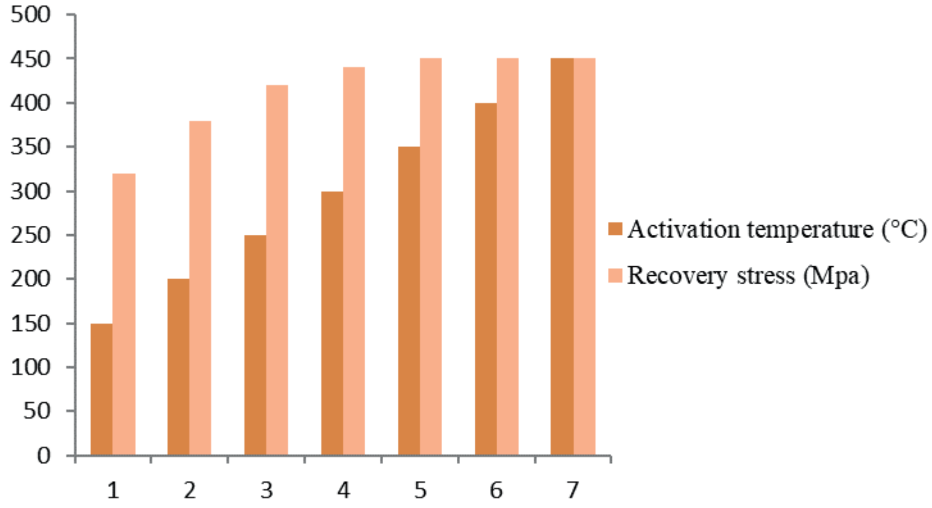

***Figure 16** Recovery stress with respect to an activation temperature*

reinforcement, the strain gauges were attached to Fe-SMA reinforcing bars at the mid-span. Those bars are longitudinal reinforcing bars provided into the concrete beam. Hence, Figure 15 shows the load versus strain response of the Fe-SMA reinforcement. Again, it can be stated that the Fe-SMA reinforcing bar has a lower modulus of elasticity as compared to the conventional reinforcement. When the flexural cracks occur, high strains are developed at the mid-span of the beam. The yield point of both the Fe-SMA and conventional reinforcement differs.

Now, it is obvious that at the higher activation temperatures recovery stress shows larger values. After heating the Fe-SMA at temperatures in the range of 150 - 450 °C, the recovery stress increased from 320 MPa to 450 MPa, as indicated in Figure 16. We generally do not require higher activation temperatures for concrete structures to maintain proper bonds between the concrete and Fe-SMA. This property of recovery stress is of a great interest for such adaptive Fe-SMA reinforcements in terms of diminishing the crack propagation in concrete members. We used this phenomenon of SM alloy reinforcements for actively monitoring the self-recovery of the beam. After increasing the cycle-fatigue load these activated Fe-SMAs revealed an insignificant decrease in stiffness. Perhaps, a decrease in recovery stress occurs with an increase in cyclic loads. The reversible phase transformation-induced deformations are observed at this stage..

6 Conclusions

In the present research, the feasibility of the Fe-SMA reinforcing bars, to be used as an alternative to conventional reinforcement in structural engineering, was considered. Tensile test, bend test and corrosion test were carried out on TOR steel, mild steel and Fe-SMA reinforcing bars and test results were compared. The pull-out test on concrete with TOR steel, mild steel and Fe-SMA reinforcing bars was performedto check the bond strength. The Flexural test, under the four-point bending test conditions, was performed on RC beams with conventional reinforcement, Fe-SMA reinforcement and a combination of conventional reinforcement, both experimentally and analytically in ANSYS 16, to evaluate the comparison between the conventional and Fe-SMA reinforcement, with respect to its flexural strength and too interpret the comparison between the conventional and Fe-SMA reinforcement, with respect to the stress, deformation developed in beams and fatigue properties of reinforcing. The conclusions from the above study have been drawn as follows:

Chemical test results reveal that corrosion resistance of the Fe-SMA reinforcing bars was enhanced due to the addition of silicon along with manganese and chromium in iron. The tensile strength of Fe-SMA reinforcing bars is greater than those of both mild and TOR steels, which shows that the Fe-SMA reinforcing bars would sustain severe loads for a longer time than the conventional reinforcing bars. There is no crack observed on TOR steel, mild steel and Fe-SMA reinforcing bars after a 180° bend which reveals that they are satisfactory to be used as reinforcements. The corrosion test results reveal that the Fe-SMA reinforcing bar is more corrosion resistant than the conventional reinforcement, as there was slightly red pitting observed at the cutting edge. The bond strength of Fe-SMA reinforcing bar is smaller than that of the TOR steel and mild steel. Therefore, the deformed Fe-SMA reinforcing bars should be used instead of plain Fe-SMA reinforcing bars, to achieve better bond strength. Flexural strength result reveals that the RC beam reinforced with Fe-SMA reinforcing bars can withstand in severe conditions and has a greater load-carrying capacity than the conventional reinforcing bars. There is a good agreement between the experimental and analytical results. Total deformation of an RC beam with Fe-SMA reinforcement full replacement is marginally higher than the conventional RC beam, however, it has the capability of recentering, crack vanishing and recovering due to the chemical composition of the Fe-SMA reinforcing bars. The service life of the Fe-SMA reinforcement is far longer than that of the conventional reinforcement. It is demonstrated that the conventional reinforcement in RC beam can be replaced by 50% or 100% by super elastic iron-based shape memory alloy, very effectively in terms of strength and life of the material. The Fe-SMA is a cost-effective alternative to NiTi-based alloys.

Grants and funding

The authors received no financial support for the research, authorship and/or publication of this article.

Conflicts of interest

The authors declare that they have no known competing financial interests or personal relationships that could have appeared to influence the work reported in this paper.

References

[1] SATO, A., CHISHIMA, E., SOMA, K., MORI, T. Shape memory effect in y transformation in Fe-30Mn-1Si alloy single crystals. *Acta Metallurgica* [online]. 1982, **30**(6), p. 1177-1183. ISSN 0001-6160. Available from: https://doi.org/10.1016/0001-6160(82)90011-6

[2] OTSUKA, H. Fe-Mn-Si based shape memory alloys. *MRS Online Proceedings Library* [online]. 1991, **246**(1), p. 309-320. eISSN 1946-4274. Available from: https://doi.org/10.1557/PROC-246-309

[3] DUERIG, T. W., PELTON, A. R. Ti-Ni shape memory alloys. In: *Materials properties handbook: titanium alloys*. WELSCH, G., BOYER, R., COLLINGS, E. W. (eds.). American Society for Metals, 1994. ISBN 0-87170-481-1, p. 1035-1048.

[4] CROCI, G., BONCI, A., VISKOVIC, A. Use of shape memory alloy devices in the basilica of St Francis of Assisi. In: Final Workshop of ISTECH Project - Shape Memory Alloy Devices for Seismic Protection of Cultural Heritage Structures: proceedings. 2000. p. 110-113.

[5] INDIRLI, M., CASTELLANO, M. G., CLEMENTE, P., MARTELLI, A. Demo-application of shape memory alloy devices: the rehabilitation of the S. Giorgio Church Bell-Tower. In: SPIE's 8th Annual International Symposium on Smart Structures and Materials: proceedings [online]. Vol. 4330. 2001. p. 262-272. Available from: https://doi.org/10.1117/12.434126

[6] MAZZOLANI, F. M., MANDARA, A. Modern trends in the use of special metals for the improvement of historical and monumental structures. *Engineering Structures* [online]. 2002, **24**(7), p. 843-856. ISSN 0141-0296, eISSN 1873-7323. Available from: https://doi.org/10.1016/S0141-0296(02)00023-8

[7] SONG, G., MO, Y. L., Increasing concrete structural survivability using smart materials. A proposal submitted to Grants to Enhance and Advance Research (GEAR). Houston: University of Houston, 2003.

[8] FUKUTA, T., IIBA, M., KITAGAWA, Y., SAKAI, Y. Experimental study on stress-strain property of shape memory alloy and its application to self-restoration of structural members. In: 13th World Conference on Earthquake Engineering: proceedings. 2004. Paper No. 610.

[9] LI, H., LIU, M., OU, J. Vibration mitigation of a stay cable with one shape memory alloy damper. *Structural Control and Health Monitoring* [online]. 2004, **11**(1), p. 1-36. eISSN 1545-2263. Available from: https://doi.org/10.1002/stc.29

[10] JANKE, L., CZADERSKI, C., MOTAVALLI, M., RUTH, J. Applications of shape memory alloys in civil engineering structures - overview, limits and new ideas. *Materials and Structures* [online]. 2005, **38**, p. 578-592. ISSN 1359-5997, eISSN 1871-6873. Available from: https://doi.org/10.1007/BF02479550

[11] SONG, G., MA, N., LI, H.-N. Applications of shape memory alloys in civil structures. *Engineering Structures* [online]. 2006, **28**(9), p. 1266-1274. ISSN 0141-0296, eISSN 1873-7323. Available from: https://doi.org/10.1016/j.engstruct.2005.12.010

[12] ALAM, M. S., YOUSSEF, M. A., NEHDI, M. Analytical prediction of the seismic behaviour of super elastic shape memory alloy reinforced concrete elements. *Engineering Structures* [online]. 2008, **30**(12), p. 3399-3411. ISSN 0141-0296, eISSN 1873-7323. Available from: https://doi.org/10.1016/j.engstruct.2008.05.025

[13] EL-BORGI, S., NEIFAR, M., BEN JABEUR, M., CHERIF, D., SMAOUI, H. Use of copper shape memory alloys in retrofitting historical monuments. *Smart Structures and Systems* [online]. 2008, **4**(2), p. 247-259. ISSN 1738-1584, eISSN 1738-1991. Available from: https://doi.org/10.12989/sss.2008.4.2.247

[14] INDIRLI, M., CASTELLANO, M. Shape memory alloy devices for the structural improvement of masonry heritage structures. *International Journal of Architectural Heritage* [online]. 2008, **2**(2), p. 93-119. ISSN 1558-3058, eISSN 1558-3066. Available from: https://doi.org/10.1080/15583050701636258

[15] KUMAR, P. K., LAGOUDAS, D. C. Introduction to shape memory alloys. In: *Shape memory alloys modeling and engineering applications* [online]. LAGOUDAS, D. C. (ed.). New York, NY: Springer, 2008. ISBN 978-0-387-47684-1, eISBN 978-0-387-47685-8, p. 1-51. Available from: https://doi.org/10.1007/978-0-387-47685-8

[16] MARUYAMA, T., KURITA, T., KOZAKI, S., ANDOU, K., FARJAMI, S., KUBO, H. Innovation in producing crane rail fishplate using Fe-Mn-Si-Cr based shape memory alloy. *Materials Science and Technology* [online]. 2008, **24**(8), p. 908-912. ISSN 0267-0836, eISSN 1743-2847. Available from: https://doi.org/10.1179/174328408X302585

[17] KUANG. Y.-CH., OU, J.-P. Passive smart self-repairing concrete beams by using shape memory alloy wires and fibers containing adhesives. *Journal of Central South University of Technology* [online]. 2008, **15**, p. 411-417. ISSN 2095-2899, eISSN 2227-5223. Available from: https://doi.org/10.1007/s11771-008-0077-9

[18] NASCIMENTO, M. M. S. F., DE ARAUJO, C. J., DE ALMEIDA, L. A. L., DA ROCHA NETO, J. S., LIMA, A. M. N. A mathematical model for the strain -temperature hysteresis of shape memory alloy actuators. *Materials and Design* [online]. 2009, **30**(3), p. 551-556. ISSN 0261-3069. Available from: https://doi.org/10.1016/j.matdes.2008.05.062

[19] ALSALEH, R., CASCIATI, F., EL-ATTAR, A. AND EI-HABBAL, I. M., Experimental investigation toward an SMA retrofitting application. In: 5th European Workshop on Structural Health Monitoring: proceedings. 2010. ISBN 978-1605950242, p. 1116-1123.

[20] KHALOO, A. R., ESHGHI, I., PIRAN, P. Study of behavior of reinforced concrete beams with smart rebar using finite element modeling. *International Journal of Civil Engineering* [online]. 2010, **8**(3), p. 221-231. ISSN 1735-0522. Available from: http://ijce.iust.ac.ir/article-1-166-en.html

[21] NEHDI, M., SHAHRIA ALAM, M., YOUSSEF, M. A. Development of corrosion-free concrete beam column joint with adequate seismic energy dissipation. *Engineering Structures* [online]. 2010, **32**, p. 2518-2528. ISSN 0141-0296, eISSN 1873-7323. Available from: https://doi.org/10.1016/j.engstruct.2010.04.020

[22] MARUYAMA, T., KUBO, H., OHKATA, I., TSUCHIYA, K., MIYAZAKI, S. *Ferrous (Fe-based) shape memory alloys (SMAs): properties, processing and applications*. Cambridge: Woodhead Publishing Limited, 2011. p. 141-159.

[23] SPEICHER, M. S., DESROCHES, R., LEON, R. T. Experimental results of a NiTi shape memory alloy (SMA)-based recentering beam-column connection. *Engineering Structures* [online]. 2011, **33**(9), p. 2448-2457. ISSN 0141-0296, eISSN 1873-7323. Available from: https://doi.org/10.1016/j.engstruct.2011.04.018

[24] OZBULUT, O. E., HURLEBAUS, S., DESROCHES, R. Seismic response control using shape memory alloys: a review. *Journal of Intelligent Material Systems and Structures* [online]. 2011, **22**(14), p. 1531-1549. ISSN 1045-389X, eISSN 1530-8138. Available from: https://doi.org/10.1177/1045389X11411

[25] PAUL, N. K., SAHA, S. Improvement of load-carrying capacity of a RCC t-beam bridge longitudinal girder by replacing steel bars with SMA Bars. *International Journal of Civil and Environmental Engineering*. 2017, **11**(7), p. 1008-1012. ISSN 2227-2763, eISSN 2077-1258.

[26] ABDULRIDHA, A., PALERMO, D., FOO, S., VECCHIO, F. J. Behavior and modeling of superelastic shape memory alloy reinforced concrete beams. *Engineering Structures* [online]. 2012, **49**, p. 893-904. ISSN 0141-0296, eISSN 1873-7323. Available from: https://doi.org/10.1016/j.engstruct.2012.12.041

[27] SHAHRIA ALAM, M., MONI, M., TESFAMARIAM, S. Seismic over strength and ductility of concrete buildings reinforced with superelastic shape memory alloy rebar. *Engineering Structures* [online]. 2012, **34**, p. 8-20. ISSN 0141-0296, eISSN 1873-7323. Available from: https://doi.org/10.1016/j.engstruct.2011.08.030

[28] MUNTASIR BILLAH, A. H. M., SHAHRIA ALAM, M. Seismic performance of concrete columns reinforced with hybrid shape memory alloy (SMA) and fiber Reinforced polymer (FRP) bars. *Construction and Building Materials* [online]. 2012, **28**(1), p. 730-742. ISSN 0950-0618, eISSN 1879-0526. Available from: https://doi.org/10.1016/j.conbuildmat.2011.10.020

[29] CHOI, E., PARK, S.-H., CHO, B.-S., HUI, D. Lateral reinforcement of welded SMA rings for reinforced concrete columns. *Journal of Alloys and Compounds* [online]. 2013, **577**(S1), p. S756-S759. ISSN 0925-8388, eISSN 1873-4669. Available from: https://doi.org/10.1016/j.jallcom.2012.02.135

[30] ZAFAR, A., ANDRAWES, B. Seismic behavior of shape memory composite bars in RC moment frames. In: 15th World Conference on Earthquake Engineering: proceedings. 2012.

[31] BAJORIA, K. M., WANKHADE, R. L. Free vibration of simply supported piezolaminated composite plates using finite element method. *Advanced Materials Research* [online]. 2012, **587**, p 52-56. ISSN 1662-8985. Available from: https://doi.org/10.4028/www.scientific.net/AMR.587.52

[32] WANKHADE, R. L., BAJORIA, K. M. Stability of simply supported smart piezolaminated composite plates using finite element method. In: International Conference on Advances in Aeronautical and Mechanical Engineering - AME 2012: proceedings. Vol. 1. 2012. ISBN 978-981-07-2683-6, p. 14-19.

[33] WANKHADE, R. L., BAJORIA, K. M. Free vibration and stability analysis of piezolaminated plates using finite element method. *Smart Materials and Structures* [online]. 2013, **22**(12), 125040. ISSN 0964-1726, eISSN 1361-665X. Available from: https://doi.org/10.1088/0964-1726/22/12/125040

[34] WANKHADE, R. L., BAJORIA, K. M. Buckling analysis of piezolaminated plates using higher order shear deformation theory. *International Journal of Composite Materials* [online]. 2013, **3**(4), p. 92-99. ISSN 2166-479X, eISSN 2166-4919. Available from: https://doi.org/10.5923/j.cmaterials.20130304.02
[35] JALAEEFAR, A., ASGARIAN, B. Experimental investigation of mechanical properties of nitinol, structural steel and their hybrid component. *Journal of Materials in Civil Engineering* [online]. 2013, **25**(10), p. 1498-1505. ISSN 0899-1561, eISSN 1943-5533. Available from: https://doi.org/10.1061/(ASCE)MT.1943-5533.0000701
[36] NAZIM, O.-B., BOUZID, A.-H., BRAILOVSKI, V. On the use of shape memory alloy studs to recover load loss in bolted joints. *Journal Pressure Vessel Technology* [online]. 2013, **135**(2), PVT-11-1178. ISSN 0094-9930, eISSN 1528-8978. Available from: https://doi.org/10.1115/1.4023416
[37] CLADERA, A., WEBER, B., LEINENBACH, C., CZADERSKI, C., SHAHVERDI, M., MOTAVALLI, M. Iron-based shape memory alloys for civil engineering structures: an overview. *Construction and Building Materials* [online]. 2014, **63**, p. 281-293. ISSN 0950-0618, eISSN 1879-0526. Available from: https://doi.org/10.1016/j.conbuildmat.2014.04.032
[38] CZADERSKI, C., SHAHVERDI, M., BRONNIMANN, R., LEINENBACH, C., MOTAVALLI, M. Feasibility of iron-based shape memory alloy strips for prestressed strengthening of concrete structures. *Construction and Building Materials* [online]. 2014, **56**, p. 94-105. ISSN 0950-0618, eISSN 1879-0526. Available from: https://doi.org/10.1016/j.conbuildmat.2014.01.069
[39] SEPULVEDA, J., BOROSCHEK, R., HERRERA, R., MORONI, O., SARRAZIN, M. Steel beam -column connection using copper-based shape memory alloy dampers. *Journal of Constructional Steel Research* [online]. 2008, **64**(4), p. 429-435. ISSN 0143-974X, eISSN 1873-5983. Available from: https://doi.org/10.1016/j.jcsr.2007.09.002
[40] MALAGISI, S., MARFIA, S., SACCO, E., TOTI, J. Modeling of smart concrete beams with shape memory alloy actuators. *Engineering Structures* [online]. 2014, **75**, p. 63-72. ISSN 0141-0296, eISSN 1873-7323. Available from: https://doi.org/10.1016/j.engstruct.2014.05.035
[41] CZADERSKI, CH., SHAHVERDI, M., MOTAVALLI, M., WEBER, B. Iron-based shape memory alloys (Fe-SMA) - a new material for prestressing concrete structure. In: 3rd Conference on Smart Monitoring, Assessment and Rehabilitation of Structures SMAR 2015: proceedings. 2015.
[42] BAJORIA, K. M., WANKHADE, R. L. Vibration of cantilever piezolaminated beam with extension and shear mode piezo actuators. In: SPIE Smart Structures and Materials + Nondestructive Evaluation and Health Monitoring: proceedings. Vol. 9431. 2015. 943122. Available from: https://doi.org/10.1117/12.2084271
[43] WANKHADE, R. L., BENDINE, K. Vibration control of FGM piezoelectric plate based on LQR genetic search. *Open Journal of Civil Engineering* [online]. 2016, **6**(1), p. 1-7. ISSN 2164-3164, eISSN 2164-3172. Available from: https://doi.org/10.4236/ojce.2016.61001
[44] WANKHADE, R. L., BAJORIA, K. M. Shape control and vibration analysis of piezolaminated plates subjected to electro-mechanical loading. *Open Journal of Civil Engineering* [online]. 2016, **6**(3), p. 335-345. ISSN 2164-3164, eISSN 2164-3172. Available from: https://doi.org/10.4236/ojce.2016.63028
[45] NAGASHIMA, N., SAWAGUCHI, T., OGAWA, K. Fatigue properties of Fe-28Mn-6Si-5Cr-0.5Nbc alloy. *Procedia Structural Integrity* [online]. 2016, **2**, p. 1435-1442. eISSN 2452-3216. Available from: https://doi.org/10.1016/j.prostr.2016.06.182
[46] WANKHADE, R. L., BAJORIA, K. M. Numerical optimization of piezolaminated beams under static and dynamic excitations. *Journal of Science: Advanced Materials and Devices* [online]. 2017, **2**(2), p. 255-262. ISSN 2468-2284, eISSN 2468-2179. Available from: https://doi.org/10.1016/j.jsamd.2017.03.002
[47] BENDINE, K., WANKHADE, R. L. Optimal shape control of piezolaminated beams with different boundary condition and loading using genetic algorithm. *International Journal of Advanced Structural Engineering* [online]. 2017, **9**(4), p. 375-384. ISSN 2008-3556, eISSN 2008-6695. Available from: https://doi.org/10.1007/s40091-017-0173-x
[48] WANKHADE, R. L., BAJORIA, K. M. Vibration analysis of piezolaminated plates for sensing and actuating applications under dynamic excitation. *International Journal of Structural Stability and Dynamics* [online]. 2019, **19**(10), 1950121. ISSN 0219-4554, eISSN 1793-6764. Available from: https://doi.org/10.1142/S0219455419501219
[49] WANKHADE, R. L., BAJORIA, K. M. Vibration attenuation and dynamic control of piezolaminated plates with coupled electromechanical actuation. *Archive of Applied Mechanics* [online]. 2021, **91**, p. 411-426. ISSN 0939-1533, eISSN 1432-0681. Available from: https://doi.org/10.1007/s00419-020-01780-6
[50] IS 383: 1970. Specification for coarse and fine aggregates from natural sources for concrete.
[51] IS 11309: 1985. Method of conducting pull-out test on anchor bars and rock bolts.
[52] IS 9879: 1998. Method for emission spectrometric analysis of austenitic and ferritic stainless steels point to plane technique.
[53] IS 9103: 1999. Concrete admixtures-specifications.
[54] IS 1786: 2008. Indian standard code for high strength deformed steel bars and wires for concrete reinforcement.
[55] IS 10262: 2009. Concrete mix proportioning-guidelines.

[56] ASTM B117: 2011. Test conditions, method and application.
[57] IS 12269: 2013. Ordinary portland cement. 53 grade-specifications.
[58] IS 516 (Part-1 Sec-I): 2021. Compressive, flexural and split tensile strength.
[59] ASTM A370: 2021. Standard test methods and definitions for mechanical testing of steel products.